Measuring Cortical Neurite-Dispersion and Perfusion in Preterm-Born Adolescents Using Multi-modal MRI

Andrew Melbourne[1], Zach Eaton-Rosen[1], David Owen[1], Jorge Cardoso[1], Joanne Beckmann[2], David Atkinson[3], Neil Marlow[2], and Sebastien Ourselin[1]

[1] Centre for Medical Image Computing, University College London, UK
[2] Academic Neonatology, EGA UCL Institute for Women's Health, London, UK
[3] Medical Physics, University College Hospital, London, UK

Abstract. As a consequence of a global increase in rates of extremely preterm birth, predicting the long term impact of preterm birth has become an important focus of research. Cohorts of extremely preterm born subjects studied in the 1990s are now beginning to reach adulthood and the long term structural alterations of disrupted neurodevelopment in gestation can now be investigated, for instance with magnetic resonance (MR) imaging. Disruption to normal development as a result of preterm birth is likely to result in both cerebrovascular and microstructural differences compared to term-born controls. Of note, arterial spin labelled MRI provides a marker of cerebral blood flow, whilst multi-compartment diffusion models provide information on the cerebral microstructure, including that of the cortex. We apply these techniques to a cohort of 19 year-old adolescents consisting of both extremely-preterm and term-born individuals and investigate the structural and functional correlations of these MR modalities. Work of this type, revealing the long-term structural and functional differences in preterm cohorts, can help better inform on the likely outcomes of contemporary extremely preterm newborns and provides an insight into the lifelong effects of preterm birth.

1 Introduction

Very preterm birth (birth at less than 32 weeks completed gestational age) occurs at a time of rapid neurological development supported by changes in blood flow and distribution. Preterm birth leads to an increased risk of adverse neurodevelopmental outcome [1] and this is believed to be related to delay or disruption to normal developmental and subsequent longterm deficits. Investigation of the long term impacts of prematurity in early adulthood allows us to infer the impact of early injury on later functional development. The effect of preterm birth on the cardiovascular system has recently been investigated [2] where raised blood pressure and increased cardiac wall thickness were observed. These effects are thought to be related to the long term impact of the early switch from a placental circulation to a driven pulmonary circulation, although this is likely to be complicated by intrauterine infection, hypoxia and poor postnatal organ

N. Navab et al. (Eds.): MICCAI 2015, Part III, LNCS 9351, pp. 72–79, 2015.
DOI: 10.1007/978-3-319-24574-4_9

growth. The consequential impact of preterm birth on the cerebrovascular system is an open area of research and combined measurement of both flow and cortical architecture are likely to be important in establishing both the impact of prematurity on function and also providing early evidence of cerebrovascular disease in adulthood.

Arterial Spin Labelled (ASL) MRI has achieved some success in recent years, linked to the increased availability of 3T MRI, as an endogenous tracer technique for measuring blood flow and perfusion [3]. The technique has found many applications and here we apply the technique to investigating the long term influence of preterm birth and relate this to cortical microstructure as assessed by diffusion weighted MRI (DWI). Measurement of changes to cerebral blood flow (CBF) allows investigation of the functional properties of the tissue. Accurate measurement of alterations in brain perfusion as a result of preterm birth may have substantial benefit for predicting lifelong risk of vascular disorders and thus preventative steps can be taken at an early age. Combined with multi-compartment diffusion imaging, the joint role of ASL and microstructure can be investigated and in this work we make this possible by combining two such modalities.

Substantial changes in architecture and appearance occur in the cortex during the last 10 weeks of gestation. The appearance of intra-cortical arborisation and new cortico-cortical connections can be observed using diffusion weighted MRI (DWI). Recent biophysically motivated models of grey and white matter diffusion characteristics can be used to observe these changes *in vivo* [4]. These structural changes occur in tandem with changes to the microvascular environment and preterm birth results in much of this development taking place in altered developmental conditions. A combination of focal brain tissue injury and developmental disturbances is thought to be responsible for many of the functional deficits seen at later ages [5] and would be reflected in structural and function changes measured using a range of MR modalities.

There is some support for the theory that oxygen delivery is limited by the propensity of oxygen to diffuse through extra-vascular tissue and that this explains some of the relationships observed using arterial spin labelled and blood-oxygenation level dependent MRI [6,7]. The cortical microenvironment observed by the diffusion of water in DWI is also the environment that provides a barrier to oxygen diffusion and thus it is plausible that a relationship would be observed. Specifically, this would imply that the local structure and local tissue composition relate to blood delivery to the cortex and specifically that increased cortical orientation dispersion (and thus a more complex local tissue arrangement) would correlate with increased local cerebral, and thus cortical, blood flow.

In this work, we use a novel modified diffusion model-fit that makes use of T2-weighted images to separate contributions from tissue and free isotropic volume fractions and use this to investigate the relationship of these parameters with the measured CBF from ASL. This is the first time that correlations of this type have been shown in this extremely-preterm born adolescent cohort.

2 Methods

Data. Data was collected from 43 preterms (born at less than 26 weeks completed gestation) and 21 term-born adolescents at 19 years of age. On a Philips 3T Achieva we acquired Pseudo-Continuous ASL (PCASL) for 30 control-label pairs with PLD=1800ms+41ms/slice, label duration (τ)=1650ms (3x3x5mm). Acquisition was carried out using 2D EPI in the same geometry as the DWI ensuring similar levels of distortion. Diffusion weighted data was acquired across four b-values at $b = \{0, 300, 700, 2000\} s.mm^{-2}$ with $n = \{4, 8, 16, 32\}$ directions respectively at TE=70ms (2.5x2.5x3.0mm). T2 weighted data was acquired in the same space as the diffusion imaging with five echo times at TE={40,50,85,100,150}ms. In addition we acquired a 3D T1-weighted volume at 1mm isotropic resolution for obtaining a segmentation and region labels [8].

Arterial Spin Labelled MRI. PCASL data can be used to estimate a cerebral blood flow map (CBF) using the following relationship [3]:

$$\text{CBF} = \frac{6000\lambda}{2\alpha} \frac{e^{\text{PLD}/\text{T1}_{\text{blood}}}}{\text{T1}_{\text{blood}}(1 - e^{-\tau/\text{T1}_{\text{blood}}})} \frac{(S_C - S_L)}{S_{PD}} [\text{ml}/100g/\text{min}] \qquad (1)$$

where λ is the plasma/tissue partition coefficient (0.9ml/g), PLD the post-labelling delay after the end of the bolus, T1_{blood} the blood T1 value ($1650ms$), α the labelling efficiency (0.85) and τ the labelling pulse duration.

Multi-compartment Diffusion Weighted Imaging. We fit a multi- compartment signal model to the multi-shell data using non-linear least squares [9]. We fit the model simultaneously to the diffusion weighted and T2 data, treating the T2 data as unweighted diffusion data with variable echo time. We provide a modification of the method of [9] to explicitly incorporate a two-compartment T2 distribution allowing correction of volume fractions in regions of mixed T2, such as voxels containing both GM and CSF which are of interest for this work.

$$S(b, \mathbf{x}) = S_0 \left[v_{iso} e^{-bd_{iso}} e^{-\text{TE}/\text{T2}_{iso}} + (v_{in} A_{in} + v_{ex} A_{ex}) e^{-\text{TE}/\text{T2}_{tis}} \right] \qquad (2)$$

The signal model attributes the grey matter signal measured by DWI to three compartments; an intra-neurite space, with volume fraction v_{in} and signal modelled by $A_{in}(\gamma, \mathbf{x}, \theta, \phi, d_{||})$, and an extra-neurite space, with volume fraction v_{ex} with signal modelled by $A_{ex}(v_{in}, \gamma, \mathbf{x}, \theta, \phi, d_{||})$ and a free-isotropic space with volume fraction, v_{iso} modelled as a function of isotropic diffusivity d_{iso} [10]. The two angular parameters θ and ϕ define the principal diffusion direction whilst $d_{||}$ and d_{iso} describe parallel (to the principal direction) and isotropic diffusivities respectively. Given the experimental b-value, b, and gradient direction, $\mathbf{x}$, the signal from the intra and extra-neurite spaces is coupled by a specific distribution, $f(\mathbf{n}, \gamma)$, which is assumed to represent axonal dispersion; formally a Watson distribution of oblateness γ, varying between 0, for highly oriented axons, up to

1 when there is no preferred structural orientation [9]. This distribution couples the intra and extra neurite spaces. The multi-compartment diffusion fitting routine above can be enhanced by the inclusion of T2 relaxometry data. In this case we give the algorithm additional information, ostensibly to give a higher precision estimate of the v_{iso} volume fraction. Analysis is simplified by only varying the TE of the b0 images, in which case the equation simplifies in the absence of diffusion-weighting to become a two-component T2 relaxometry fit and, using literature values at 3T, we fix the two T2 values to $\mathrm{T2}_{tis} = 100ms$ and $\mathrm{T2}_{iso} = 300ms$.

3 Results

3.1 Comparison of DWI with and without Additional T2 Imaging

Figure 1 shows examples of model-fitting with and without T2 weighted images on two preterm-born subjects. Figure 1, panel A illustrates differences seen in posterior white matter regions, with lower fitted isotropic volume fraction, whilst panel B illustrates less noisy fitting in regions of pure CSF, albeit in an extreme case. The inclusion of T2-weighted images helps suppress high white matter v_{iso} values and reduces noisy parameter values in regions of CSF. We use this to motivate the use of the joint model fitting technique.

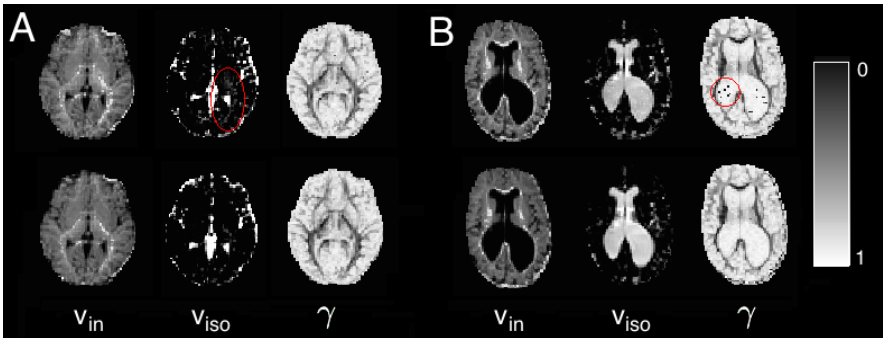

Fig. 1. Comparison of modified (top row) and non-modified (bottom row) DW model-fitting for two cases. Note the suppressed posterior white-matter v_{iso} volume fraction in case A (circled) and the reduced ventricular CSF noise for case B (v_{iso} and γ (circled)).

3.2 Comparison of Quantitative Neuroimaging Parameters

Figure 2 shows example data for a single representative control subject showing the cortical variability of the CBF and the diffusion imaging parameters. Visible is an empirical correlation between CBF and cortical orientation dispersion (γ) but not between CBF and v_{in}. A propagated labelling is also shown [8].

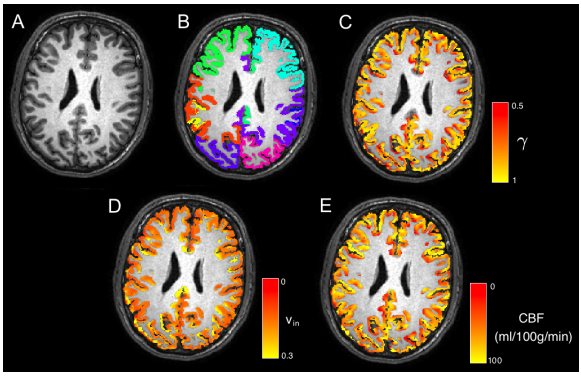

Fig. 2. Example control data. A) T1-weighted slice, B) lobe parcellation, C) cortical CBF D) cortical v_{in} E) cortical orientation dispersion γ.

Figure 3 shows the cortical distribution of diffusion characteristics and CBF. CBF values are found to be lower in the preterm cohort (48.67±5.6ml/100g/min) on average compared to their term-born counterparts (53.9 ± 7.7ml/100g/min). Grey matter volume is also lower in the preterm group with a volume of $0.578 \pm 0.06l$ compared to $0.621 \pm 0.05l$ in the term group. Distributions of parameters from diffusion imaging show increased variability: average values of v_{in} in the term-born cohort are 0.348 ± 0.08 compared to 0.380 ± 0.07 in the preterm cohort; average values of v_{iso} in the term-born cohort are 0.045 ± 0.02 compared to 0.045 ± 0.03 in the preterm cohort; and average values of γ in the term-born cohort are 0.671 ± 0.07 compared to 0.633 ± 0.07 in the preterm cohort. Of these four parameters, only the CBF and GM volume reach a significant difference for $p<0.05$ ($p=0.003$, $p=0.006$ respectively) between preterm and term groups.

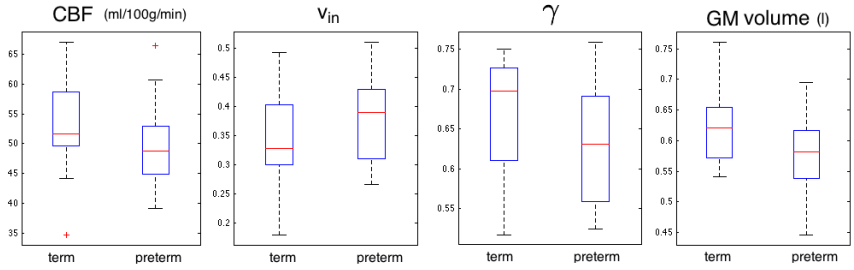

Fig. 3. Group distribution of whole-cortex average grey matter parameter values for a) CBF, b) intra-axonal volume fraction v_{in}, c) grey matter volume (litres), and d) cortical orientation dispersion γ.

3.3 Correlation of Diffusion MRI and Cerebral Blood Flow

In the absence of a known cortical diffusion to blood flow relationship, we investigate the relationship between cortical diffusion properties and CBF by comparing image similarity using Spearman's rank correlation in cortical grey matter. The distribution of correlation values between term and preterm groups is shown in Figure 4. These distributions reveal that the average correlation values are positive for both v_{in} and for γ and slightly negative for v_{iso}. Between term-born and preterm groups, paired t-tests yield insignificance for v_{in} and v_{iso} (p=0.587 and p= 0.644 respectively) and a significant difference between CBF and cortical dispersion (p=0.005). In order to account for volume effects we test for differences while correcting for volume using linear regression with a covariate, correlation for v_{in} and v_{iso} remains insignificant, whilst correlation for CBF and cortical dispersion remains highly significant (p=0.006) a weak correlation (r=0.3, p=0.014) is found between v_{iso} and γ. These results may imply that the relationship between CBF and cortical dispersion could be used as an imaging biomarker.

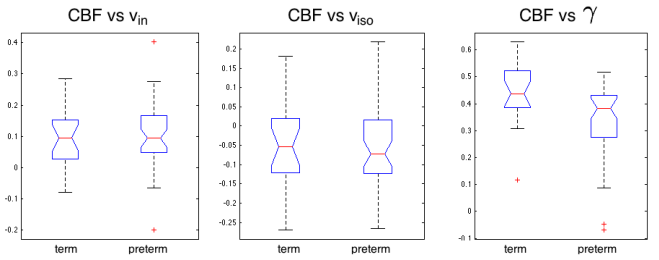

Fig. 4. Group distributions of the single-subject image correlation coefficients between CBF and grey matter parameter values for a) v_{in}, b) v_{iso} and c) γ.

We also investigate differences between frontal, temporal, parietal and occipital lobe regions (both hemispheres combined). Label-based results are shown for the four major lobes in Figure 5. The highest correlations between CBF and γ are seen in the parietal lobe and the pattern is consistent across lobes for both groups. These results are commensurate with a theory of blood delivery governed by the diffusivity of the local environment to extra-capillary oxygen.

4 Discussion

We have shown that advanced diffusion model fitting and arterial spin labelled MRI can be used to investigate the cerebral cortex and that CBF values derived from ASL MRI correlate strongly with measures of cortical orientation dispersion found from DWI. Additionally we have shown that this relationship is different between preterm and term born 19 year olds, which possibly reflects long term

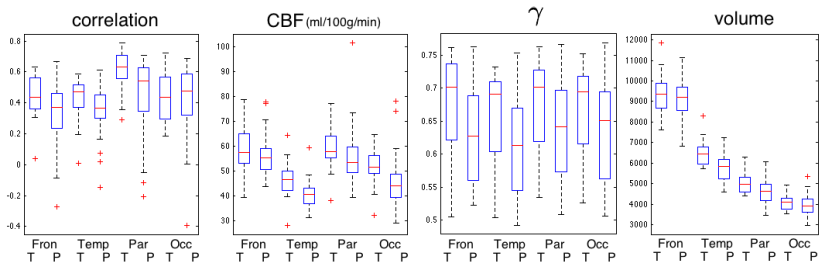

Fig. 5. Group distributions for a) the spatial correlation coefficient between CBF and γ b) CBF, c) γ and d) lobe volume for frontal (fron), temporal (temp), parietal (par) and occipital (occ) lobes (P=preterm, T=term-born).

differences in cortical architecture as a result of being born extremely premature. Including volumetric data we find that subjects in the preterm cohort have significantly reduced GM volume, but that this does not seem to influence the parametric results obtained. This is despite GM volume reduction increasing partial voluming in both the CBF and DWI parameter estimates. This effect is to some extent mitigated by the multi-compartment DWI model and its effect in ASL is unclear and confounded by global volume differences that affect CBF estimates via transit times and tissue type (T1) effects. Erring on the side of caution, the correlations we observe may thus not be causal in nature.

The combination of DWI and multi-echo T2 weighted imaging is novel and allows more robust model-fitting and has the potential to enable new models to be more accurately fitted. Future work will use this model in combination with ASL to make predictions about functional development and develop vascular biomarkers in preterm children. Once again, the combination of measurements in this work: the acquisition of widely available multi-shell DWI, multi-echo T2 imaging and CBF data within clinically feasible time frames is important and will encourage research into the generation of new predictive structural biomarkers that have a tangible physical link to neuronal structure and function.

One interesting observation for fitting of this type is that the v_{iso} estimates fitted from the diffusion model with and without varying echo-time data are complicated slightly by the different treatment of perfusion effects with and without diffusion weighting. If these can be neglected, improved model-fitting performance can be achieved; conversely, if these effects cannot be neglected this methodology opens the door to more elaborate models of MR measurement.

The analysis in this work can be developed further by acquiring more sophisticated, albeit time-consuming, multi inversion-time ASL experiments. Furthermore, although they are notoriously difficult, cortical thickness measurements could be used to assess CBF as a function of cortical tissue volume in addition to local structural differences.

In conclusion, we have shown that MRI measurement of cortical microstructure can be linked to indices of cerebral perfusion. Work of this type, linking functional performance with structural measurement; is particularly salient

for preterm-born cohorts for which accurate prediction of function is crucial to providing effective intervention. The investigation of the long term sequelae of extreme prematurity will help inform early support and intervention for those infants being born extremely premature now.

Acknowledgements. We would like to acknowledge the MRC, the National Institute for Health Research (NIHR), the EPSRC (EP/H046410/1) and the UCLH/UCL CBRC Strategic Investment Award (Ref. 168).

References

1. Costeloe, K.L., Hennessy, E.M., Haider, S., Stacey, F., Marlow, N., Draper, E.S.: Short term outcomes after extreme preterm birth in england: comparison of two birth cohorts in, and (the epicure studies). BMJ 345, e7976 (1995)
2. Lewandowski, A.J., Augustine, D., Lamata, P., Davis, E.F., Lazdam, M., Francis, J., McCormick, K., Wilkinson, A.R., Singhal, A., Lucas, A., Smith, N.P., Neubauer, S., Leeson, P.: Preterm heart in adult life: cardiovascular magnetic resonance reveals distinct differences in left ventricular mass, geometry, and function. Circulation 127(2), 197–206 (2013)
3. Alsop, D.C., Detre, J.A., Golay, X., Günther, M., Hendrikse, J., Lu, H., Macintosh, B.J., Parkes, L.M., Smits, M., van Osch, M.J.P., Wang, D.J.J., Wong, E.C., Zaharchuk, G.: Recommended implementation of arterial spin-labeled perfusion mri for clinical applications: A consensus of the ismrm perfusion study group and the european consortium for asl in dementia. Magn. Reson. Med. (April 2014)
4. Eaton-Rosen, Z., Melbourne, A., Orasanu, E., Cardoso, M.J., Modat, M., Bainbridge, A., Kendall, G.S., Robertson, N.J., Marlow, N., Ourselin, S.: Longitudinal measurement of the developing grey matter in preterm subjects using multi-modal mri. Neuroimage 111, 580–589 (2015)
5. Volpe, J.J.: Brain injury in premature infants: a complex amalgam of destructive and developmental disturbances. Lancet Neurol. 8(1), 110–124 (2009)
6. Buxton, R.B., Frank, L.R.: A model for the coupling between cerebral blood flow and oxygen metabolism during neural stimulation. J. Cereb. Blood Flow Metab. 17(1), 64–72 (1997)
7. Hoge, R.D., Atkinson, J., Gill, B., Crelier, G.R., Marrett, S., Pike, G.B.: Linear coupling between cerebral blood flow and oxygen consumption in activated human cortex. Proc. Natl. Acad. Sci. U S A 96(16), 9403–9408 (1999)
8. Cardoso, M.J., Modat, M., Wolz, R., Melbourne, A., Cash, D., Rueckert, D., Ourselin, S.: Geodesic information flows: spatially-variant graphs and their application to segmentation and fusion. IEEE TMI 99 (2015)
9. Zhang, H., Schneider, T., Wheeler-Kingshott, C.A., Alexander, D.C.: Noddi: practical in vivo neurite orientation dispersion and density imaging of the human brain. Neuroimage 61(4), 1000–1016 (2012)
10. Alexander, D.C., Hubbard, P.L., Hall, M.G., Moore, E.A., Ptito, M., Parker, G.J.M., Dyrby, T.B.: Orientationally invariant indices of axon diameter and density from diffusion mri. Neuroimage 52(4), 1374–1389 (2010)